

## WHAT WE LEARNED FROM EMMA

S. Machida, ASTeC/STFC/RAL, Didcot, United Kingdom  
on behalf of the EMMA collaboration

### Abstract

After a brief introduction of FFAG accelerators, we discuss the demonstration of serpentine channel acceleration and the fast resonance crossing in non-scaling FFAGs. Then we summarise the findings from the EMMA project so far.

### INTRODUCTION

Fixed Field Alternating Gradient (FFAG) accelerators attracted attention in the 1990s as candidates for muon acceleration for a neutrino factory [1-2]. Muons have a very short lifetime (2.2  $\mu$ s in their rest frame) and the acceleration needs to be very fast to avoid the decay of too many particles in the beam. There is no time to adjust the strength of magnets in the accelerator lattice to match the beam momentum: therefore, synchrotrons are out of question. The only options for fast acceleration are either a linac (including re-circulating versions) or an FFAG [3].

An FFAG accelerator could be classified as one kind of cyclotron. It is especially similar to a synchro-cyclotron in the sense that the magnetic field strength is constant and the rf frequency is swept according to the beam momentum. Nevertheless, a significant difference from a synchro-cyclotron is the strong focusing used in the lattice: alternating field gradients (i.e. focusing and defocusing optics) reduce the beam size and orbit excursion.

Research and development efforts on FFAG accelerators, after a long dormant period following their invention and the construction of a few electron models, aimed for demonstration of proton acceleration with a newly developed rf accelerating cavity using magnetic alloy [4]. Without ramping of magnetic fields, the machine repetition rate could be faster by some orders of magnitude compared with conventional rapid cycling synchrotrons. The goal was set to demonstrate 1 kHz operation; for comparison, the fastest cycling synchrotron (ISIS at Rutherford Appleton Laboratory) achieves 50 Hz.

Regarding the beam optics, proton FFAGs that was developed in Japan at KEK and KURRI [5] followed the conventional “scaling” principle, in which the magnetic field has a profile with strength increasing as  $r^k$ , where  $k$  is a constant field index and  $r$  is the distance from the machine centre. With this scaling law, the tune is constant (independent of beam energy), thus avoiding resonance crossings during acceleration.

In parallel to the development of very rapid cycling proton FFAGs in Japan, design efforts to optimise FFAGs for muon acceleration were carried out in the US and Europe. One outcome from those efforts was the invention of the non-scaling FFAG [6-7]. For muon acceleration, the beam stays in the accelerator for only a short time. Although a non-scaling FFAG is still a circular

accelerator, so that the beam goes through the same magnetic channel several times and resonance phenomena emerge, the time scale of resonance blow up can be longer than the whole acceleration cycle. In that case, the beam will not be badly affected by resonances, and constraints on the optics design can be greatly relaxed. Machine parameters can be optimised primarily to squeeze the beam size as well as the orbit excursion.

This novel type of FFAG consists of only dipole and quadrupole magnets, resulting in a large dynamic aperture. Since this design does not follow the conventional scaling law which fixes the transverse tune throughout the acceleration, it is called a non-scaling FFAG, or more specifically a linear non-scaling FFAG.

The advantages of non-scaling FFAGs led to discussions of their application to other areas. For example, the small orbit excursion means that small magnets can be used, which has significant advantages in accelerators for proton therapy.

The biggest question was whether non-scaling FFAGs would work as designed. Although tracking simulations showed promising performance, an experiment had to be carried out to provide a convincing demonstration. The EMMA project (Electron Model for Many Applications) was initiated and construction started at Daresbury Laboratory in the UK [8-10]. Figure 1 shows the layout and Table 1 lists principal parameters.

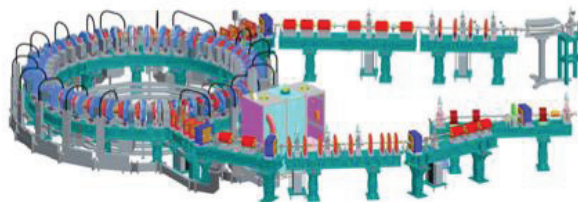


Figure 1: EMMA at Daresbury Laboratory. 10.5 MeV/c electron beams are delivered through beam transport line (bottom right) from ALICE and injected in the EMMA ring (left). The beam is extracted and its properties are measured in the diagnostic line (top right). The lattice does not have dipole magnets. Bending action comes from the shifted quadrupole magnets.

Table 1: Principal Parameters

momentum	10.5 – 20.5 MeV/c
circumference	16.57 m
number of cells	42
focusing	doublet
nominal integrated quad. field	0.402/-0.367 T
rf frequency	1.301 GHz
number of rf cavities	19
tune shift for he momentum range	0.3 to 0.1/cell
acceptance (normalized)	$3 \pi$ mm rad

### MAJOR ACHIEVEMENTS

Three main goals were set in the first stage of the EMMA commissioning. First, successful beam acceleration despite several resonance crossings should be demonstrated. During acceleration, the phase advance per unit cell changes from around  $150^\circ$  to a reasonably small value such as  $20^\circ$ . In terms of the total tune per turn, there is a change of about 10 units. In a conventional synchrotron, crossing integer tunes during acceleration is impossible because of the build-up of coherent kicks due to unavoidable field imperfections. In EMMA, on the other hand, the crossing speed is so fast that it is hoped that any significant distortion of the orbit can be avoided.

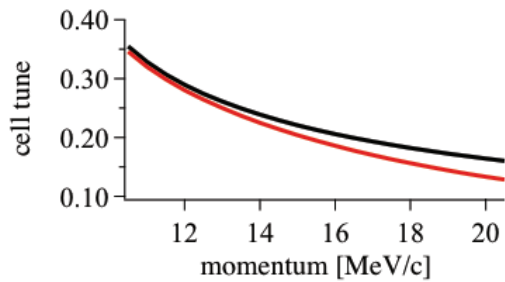


Figure 2: Cell tune as a function of momentum. Black curve is horizontal and red is vertical [9].

Second, acceleration in the so-called serpentine channel should be demonstrated. Although the machine is not isochronous, the deviation of the orbital period in the operational momentum range is much less than 1%. In addition, the lattice is adjusted such that the orbital period becomes a minimum in the middle of the acceleration and increases towards both ends; with sufficient rf voltage (and fixed frequency) a path between adjacent rf buckets is created, called a serpentine channel. It was intended in EMMA to show the existence of this channel, and to demonstrate its use for acceleration.

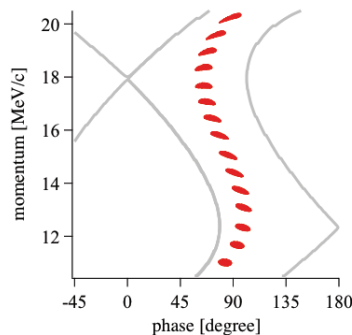


Figure 3: Serpentine channel acceleration shown in longitudinal phase space. Red dots are a stroboscopic view of accelerated beams [9].

Third, a large machine acceptance should be observed. Although a variety of applications are considered, acceleration of muons is one of major potential uses for linear non-scaling FFAGs. Muons are produced as tertiary particles and the beam emittance is huge compared with ordinary beams, even after some cooling. Very strong

focusing in FFAGs, together with a reasonable physical aperture, should give a huge acceptance.

The machine commissioning of EMMA started in 2010 and the first two goals were achieved by early 2011. Figure 4 shows the instantaneous cell tune as a function of time (the number of cells through which the beam has passed). The cell tune was measured based on the 21 consecutive beam position data processed by NAFF algorithm [11]. The cell tune as a function of momentum was measured separately using a fixed momentum beam, so that the cell tune shown in Fig. 4 could be translated into momentum.

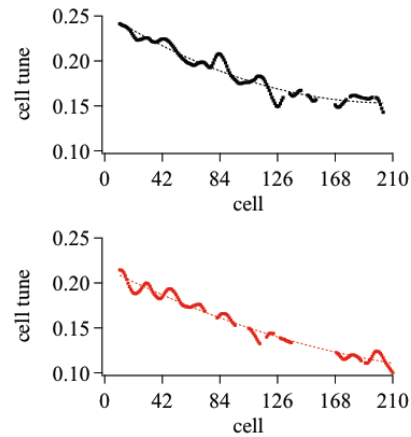


Figure 4: Horizontal (top) and vertical (bottom) cell tune when a beam is accelerated [9]. The horizontal axis is the total number of cells through which the beam has passed. One complete turn corresponds to 42 cells.

Horizontal and vertical beam positions are also measured as a function of time, as shown in Fig. 5. Although (as expected) the vertical position does not move, the beam moves horizontally during acceleration, because of dispersion. A separate set of measurements of horizontal beam position at different fixed momenta provides another calibration curve, allowing the translation of orbit position in Fig. 5 (a) to momentum.

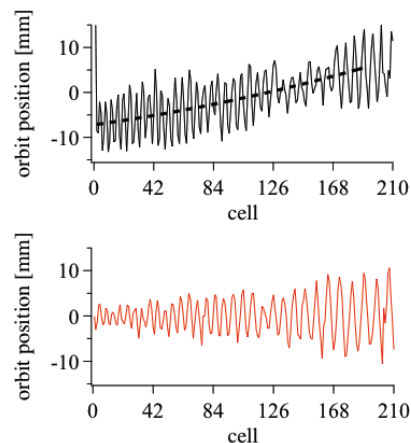


Figure 5: Horizontal (top) and vertical (bottom) orbit position during beam acceleration [9]. The horizontal axis is the total number of cells through which the beam has passed. One turn corresponds to 42 cells.

Using three different methods to calibrate the momentum, namely from horizontal and vertical cell tunes and horizontal position, the beam trajectory in longitudinal phase space can be reconstructed. Figure 6 shows that the beam was indeed accelerated in the serpentine channel.

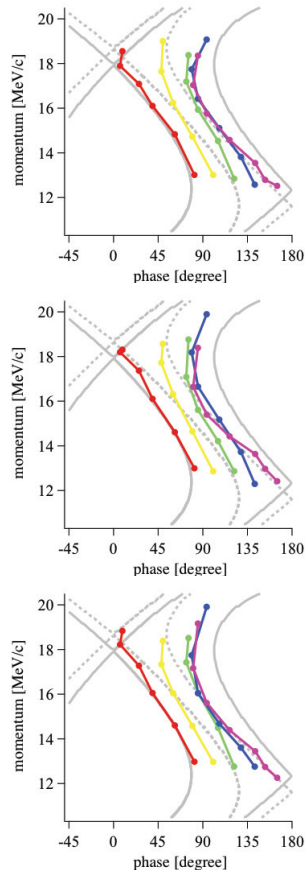


Figure 6: Longitudinal trajectories reconstructed by three different momentum calibrations [9]. Top: with horizontal orbit. Middle: with horizontal tune. Bottom: with vertical tune. Solid and dashed grey curves are separatrices at the upper and lower momentum limits, taking systematic errors into account.

Measurements of the beam orbit during acceleration, as shown in Fig. 7, suggest that the beam was not very badly affected by multiple resonance crossings during acceleration.

## WHAT WE LEARNED FROM EMMA

### *Very Small Dispersion Lattice*

When the guiding magnetic field is fixed and the beam momentum increases, orbit excursions are unavoidable. Cyclotrons intentionally use this fact to increase orbital length and satisfy isochronism.

On the other hand, one of the design goals of a linear non-scaling FFAG is to minimise the orbit excursion as much as possible by imposing very strong focusing and therefore squeezing the dispersion function. Although the momentum increases by a factor of two in EMMA, the

increase of the orbit radius is only 15 mm (at most) out of an average radius of 2.6 m. EMMA has shown the stability of a lattice with an extremely small dispersion function.

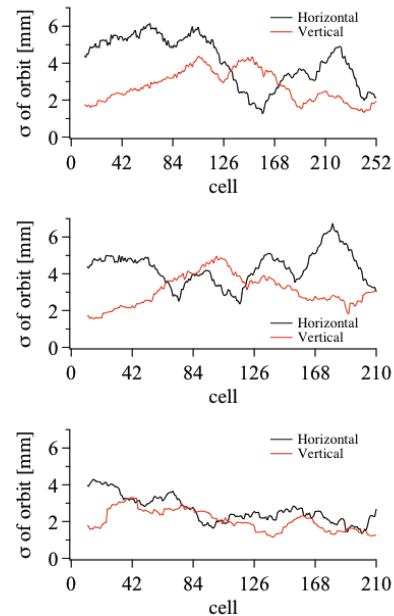


Figure 7: Standard deviation of orbit with neighbouring 21 cells [9]. Top: beam with red trajectory in Fig. 6. Middle: green trajectory in Fig. 6. Bottom: magenta trajectory in Fig. 6.

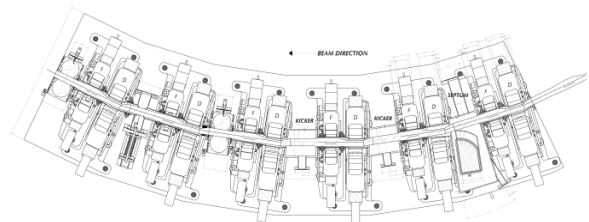


Figure 8: Vacuum chamber and lattice magnets in one sector of EMMA. It closely resembles a synchrotron lattice.

### *Almost Isochronous Lattice*

For ultra-relativistic particles, such as 10 to 20 MeV/c electrons in EMMA, isochronism can be achieved in the limit of the constant orbital length because the speed has already almost reached the speed of light. The very small dispersion helps to make the lattice almost isochronous. This allows the use of a constant frequency rf system.

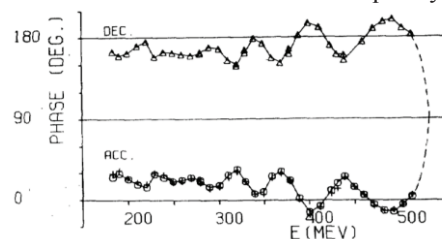


Fig. 2. Phase histories of accelerating and decelerating beams, obtained by timing an external beam.

Figure 9: Longitudinal trajectory in cyclotron from [12].

It can be claimed that, using the serpentine channel, EMMA has demonstrated a novel acceleration scheme. On the other hand, it is also true that a similar path exists in cyclotrons when isochronism is not exactly satisfied [12]: see Fig. 9.

### Very Large Transverse Acceptance

Strong focusing lattice reduces the beta functions, which together with lack of nonlinear lattice elements results in the huge acceptance, this is a requirement for muon acceleration. Although this is a very attractive feature of a linear non-scaling FFAG, some extra care does have to be taken for particles with large transverse amplitudes.

In any accelerator without chromaticity correction, the orbital period is a function of transverse amplitude: but this effect becomes more visible in an accelerator such as a non-scaling FFAG where the transverse acceptance is huge. Longitudinal phase space trajectory depends on finite transverse amplitude.

Measurements of transverse acceptance and dependence of the orbital period on transverse amplitude were made, as shown in Fig. 10 [13]. The orbital period depends linearly on the action variable, as expected from theory [14].

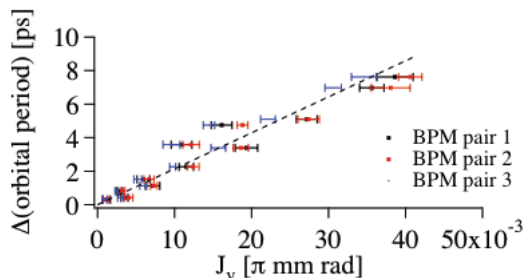


Figure 10: Shift of orbital period due to finite transverse amplitude. Three pairs of BPMs are used to measure orbital period. Results agree with the theory [14].

### Orbit Correction

A non-scaling FFAG has total tune of several units, similar to strong focusing synchrotrons. Beam position monitors (BPMs) in each cell can detect fractional betatron oscillations. A similar number of corrector magnets as BPMs are used to control the orbit. Similar orbit correction algorithms to those used in synchrotrons (such as least square method by SVD, and harmonic correction) could be employed. However, the transverse tune in a linear non-scaling FFAG is a strong function of momentum and the phase advance between BPMs and correctors is not constant, that introduces another complexity of the correction algorithm.

In EMMA, the response matrices (relating shifts in closed orbit to changes in individual correctors) at several momenta were measured. In order to find the optimum corrector setting to apply to the full momentum range, the equations  $A.c=-m$  were solved using SVD. Here,  $A$  is the  $n_{\text{mnp}} \times n_c$  response matrix,  $n_{\text{mnp}}$  is the number of BPMs times the number of momenta measured,  $n_c$  is the number of correctors, the elements of  $c$  are the corrector settings and  $m$  is the measured closed orbit distortion (COD). For example, corrector settings based on the response matrix measured at 14.3 MeV/c, 16.1 MeV/c and 18.0 MeV/c reduces the COD over a wide momentum range (from 14 to 20 MeV/c) as shown in Fig. 11.

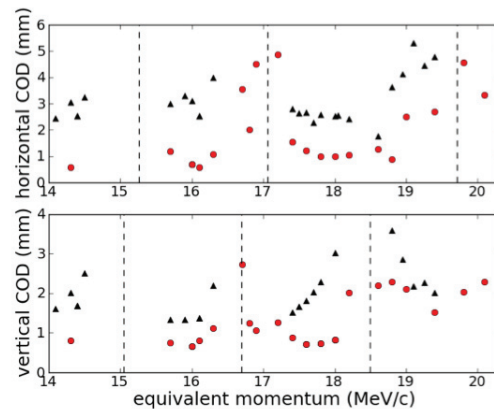


Figure 11: Amplitude of COD at different momenta. Black dots are before correction and red dots are after correction. Dashed lines show the momenta where the total tune in the ring becomes an integer.

### Integer Tune Crossing

The total tune per turn changes by several units during acceleration in a linear non-scaling FFAG: this means that the beam crosses integer tunes several times. In order to understand what is happening and also to try to minimise the effects by the crossing, we observed beam behaviour near integer tunes under controlled conditions. Simulation studies were also carried out.

When the beam comes close to an integer tune, the beam is kicked coherently and the orbit is deformed. If the beam stays close to an integer tune for long enough, the orbit shift is accumulated and eventually the beam hits the chamber. However, if the beam crosses an integer tune fast enough, the resonance may not be very harmful even if coherent motion is excited. The problem in a linear non-scaling FFAG when the beam cross integer tune is decoherence. Because of the natural chromaticity and significant momentum spread, decoherence is rather fast, which is not the case in a cyclotron.

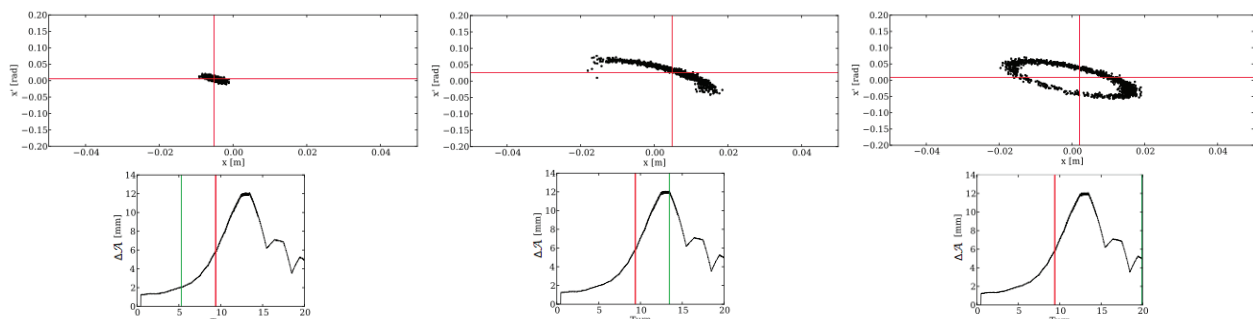


Figure 12: (Top) Transverse phase space before and after integer tune crossing by simulation. (Bottom) Oscillation amplitude of the centre of charge as function of time when the beam crosses an integer tune. The red line indicates the time when the beam goes through an integer tune. Each phase space is depicted at the time of the green line [15].

Figure 12 shows the coherent excitation when the beam cross integer tune followed by de-coherence [15]. The effective emittance becomes much larger after crossing an integer resonance.

### Injection and Extraction

The price paid for squeezing the orbit excursion and minimising the lattice circumference is a rather tight design of the injection and extraction systems, because of short straight sections. In particular, in EMMA as a scaled-down model, the space available for injection/extraction is only 210 mm, so that (for example) septum magnets with  $65^\circ$  bend are used [16].

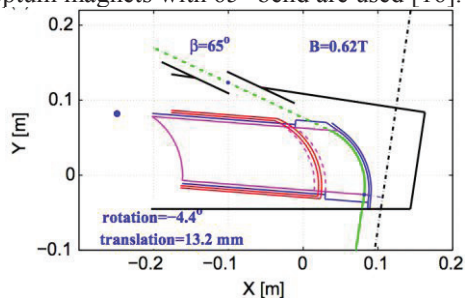


Figure 13: Injection septum (red and blue) and injection and circulation beam trajectory (green). Dashed black line is the chamber centre [16].

Obviously there is a compromise between small orbit excursions and enough space for injection and extraction. This has to be studied for each particular non-scaling FFAG design. Another example of feasible injection and extraction system for muon acceleration is in [17]. Alternative solution to ease the issue is to introduce superperiodicity and make long free space at a few places in a ring. It is not clear at the moment if such a lattice design is feasible for a linear non-scaling FFAG. Nevertheless the big success of EMMA is that both injection and extraction have been successfully accomplished despite tight space limitation.

### ACKNOWLEDGEMENTS

We greatly appreciate the assistance of the Technology Department at STFC Daresbury Laboratory during the design and construction of EMMA. Our work is supported by: the BASROC/CONFORM project (the UK

Basic Technology Fund) under Engineering and Physical Sciences Research Council (EPSRC) Grant No. EP/E032869/1; the UK Neutrino Factory project under Particle Physics and Astronomy Research Council (PPARC) Contract No. 2054; the Science and Technology Facilities Council (STFC); and the U.S. Department of Energy under Contract No. DE-AC02-98CH10886 and DE-AC02-07CH11359.

### REFERENCES

- [1] F. Mills, Linear orbit recirculators. 4<sup>th</sup> International Conference Physics Potential and Development of  $\mu^+\mu^-$  colliders, 693 (1997).
- [2] C. Johnstone, FFAG cardinal rules. *ibid*, 696 (1997).
- [3] The ISS Accelerator Working Group, M. Apollonio, *et al.*, Accelerator design concept for future neutrino facilities. *Journal of Instrumentation* **4** P07001 (2009).
- [4] M. Aiba, *et al.*, European Particle Accelerator Conference 2000, 581 (2000).
- [5] Y. Mori, International Particle Accelerator Conference 2012, 1054 (2012).
- [6] C. Johnstone, W. Wan, A. Garren, Particle Accelerator Conference 1999, 3068 (1999).
- [7] E. Keil and A. M. Sessler, *Nucl. Instrum. Methods Phys. Res.*, **A538**, 159 (2005).
- [8] R. Barlow, *et al.*, *Nucl. Instrum. Methods Phys. Res.*, **A624**, 1 (2010).
- [9] S. Machida, International Particle Accelerator Conference 2011, 951 (2011).
- [10] S. Machida, *et al.*, *Nature Physics* **8**, 243 (2012).
- [11] J. Laskar, C. Froeschle and A. Celletti, *Physica D* **56**, 253 (1992).
- [12] M. K. Craddock *et al.*, Particle Accelerator Conference 1977, 1615 (1977).
- [13] S. Machida, *et al.*, to be published.
- [14] J. S. Berg, *Nucl. Instrum. Methods Phys. Res.*, **A570**, 15 (2007).
- [15] J. Garland, PhD thesis, University of Manchester.
- [16] K. Marinov, J. A. Clarke, N. Marks and S. Tzenov, *Nucl. Instrum. Methods Phys. Res.*, **A701**, 164 (2013).
- [17] D. Kelliher *et al.*, *Int. Journal of Mod. Phys.* **A26**, Nos 10&11 1775 (2011).